We are IntechOpen, the world's leading publisher of Open Access books
Built by scientists, for scientists

1

Field Conditions of Interrogation Zone in Anticollision Radio Frequency Identification Systems with Inductive Coupling

Piotr Jankowski-Mihułowicz
Rzeszów University of Technology
Poland

1. Introduction

Passive Radio Frequency IDentification (RFID) systems with inductive coupling are the most widespread nowadays (Yan et al., 2008; Wolfram et al., 2008). These systems operate thanks to direct inductive coupling between antenna units of the communication system which consist of Read/Write Device (RWD) and electronic identifier (called a tag or transponder). The communication in transmitter – receiver set is carried out in two ways. In the first case, only one object with electronic tag can be placed in the correct working area called **interrogation zone** of the RFID system. This arrangement is called **a single identification system** or also single system. In the second case of multiple identification system, called **anticollision system**, the communication process is carried out simultaneously with multiple RFID tags. In this process, the algorithms of multi-access to the radio channel are used, what provides an effective way to distinguish simultaneously between multiple objects (Yeh et al., 2009; Dobkin & Wandinger, 2005). It should be note that synthesis procedure of interrogation zone includes the simultaneous analysis of electromagnetic field (presented in this paper), communication protocols and electric aspects of operation conditions in the process of system efficiency identification. The typical applications of anticollision RFID systems are concentrated on different economic and public activity in industry, commerce, science, medicine and others (Harrison, 2009, Donaljdson, 2009; Steden, 2005; Wyld, 2009 and 2005; Åhlström, 2005).
When determining the interrogation zone for the given automatic identification process, it is necessary to define a maximum working distance of the RFID system. This parameter determines the distance between the specified point of the RWD's and the midpoint of the tag's antenna loop. It is very important because the magnetic field generated around the RWD's antenna loop is not only medium of information signal but also provides passive tags with energy. The proper supply is essential to carry out operations of recording and reading information which is stored in the transponder's semiconductor memory (Fig. 1).
The basic parameter, which determines the working area and characterizes the maximum working distance of the RFID system, is H_{min} minimum value of magnetic field strength or more often used B_{min} **minimum value of magnetic induction** at which the correct data transmission between the RWD and the tag takes place (Jankowski-M. & Kalita, 2008). The minimum value of magnetic induction required in the process of writing data to the

Source: Radio Frequency Identification Fundamentals and Applications, Bringing Research to Practice, Book edited by: Cristina Turcu, ISBN 978-953-7619-73-2, pp. 278, February 2010, INTECH, Croatia, downloaded from SCIYO.COM

internal memory of tag ($B_{minWrite}$) is several percent larger than the value of this parameter in the process of reading ($B_{minRead}$). So the operation mode of the internal memory affects occurrence of changes in the interrogation zone. There is decreasing the maximum distance in writing mode in comparison to reading process. During the analysis of field conditions in RFID system the general case will be considered and represented by notation B_{min}.

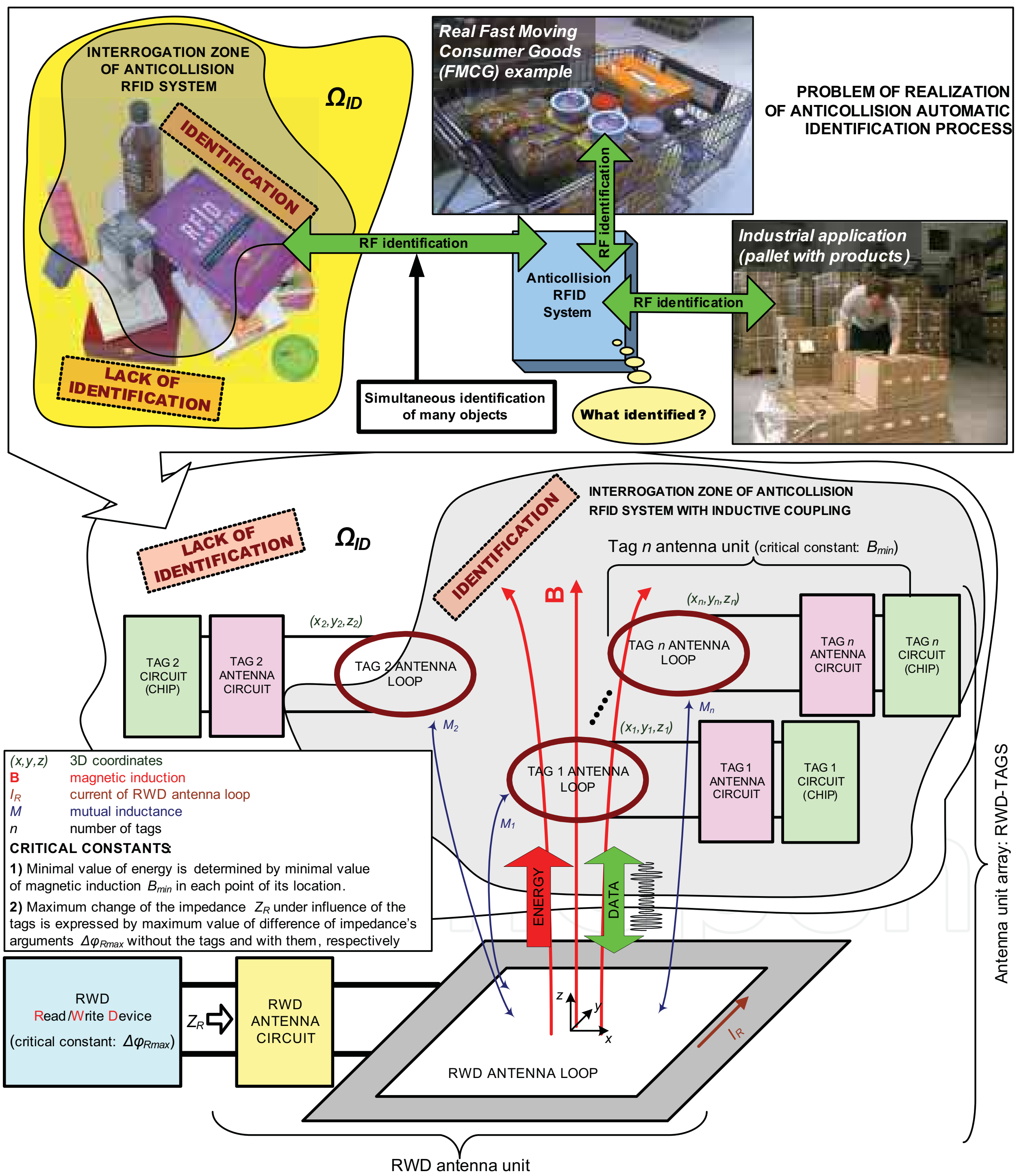

Fig. 1. Block diagram of anticollision RFID system with inductive coupling and illustration of practical automatic RFID process

The B_{min} value, which is considered individually for each transponder in a magnetic field of RWD loop (Ω_{ID} area – Fig. 1), depends on the structure and parameters of this loop but also of tag antenna. In the case of multiple identification process, it is necessary to provide all tags placed within the interrogation zone of RWD antenna with proper power. For this geometric configuration, the parameters of magnetically coupled transponders affect significantly the total loop impedance of RWD antenna and cause big changes in many parameters of its electrical circuit. In consequence, this phenomenon leads to disruption in communication with the tags which are placed within the working area but close to boundary points where the magnetic induction has the minimal value. The correct analysis of the total impedance in coupled system (consisted of RWD and tags antenna loops), and thereby analysis of changes in the magnetic field in the considered interrogation zone, allows to estimate the proper boundary of area with spatial placed multiple tags for the case of designing anticollision RFID system with inductive coupling.

2. The operating range of RFID systems with inductive coupling

In terms of emission of electromagnetic field, the RFID systems are placed in a group of radio equipment devices and they use allocated band in respective frequency range (Fig. 2).

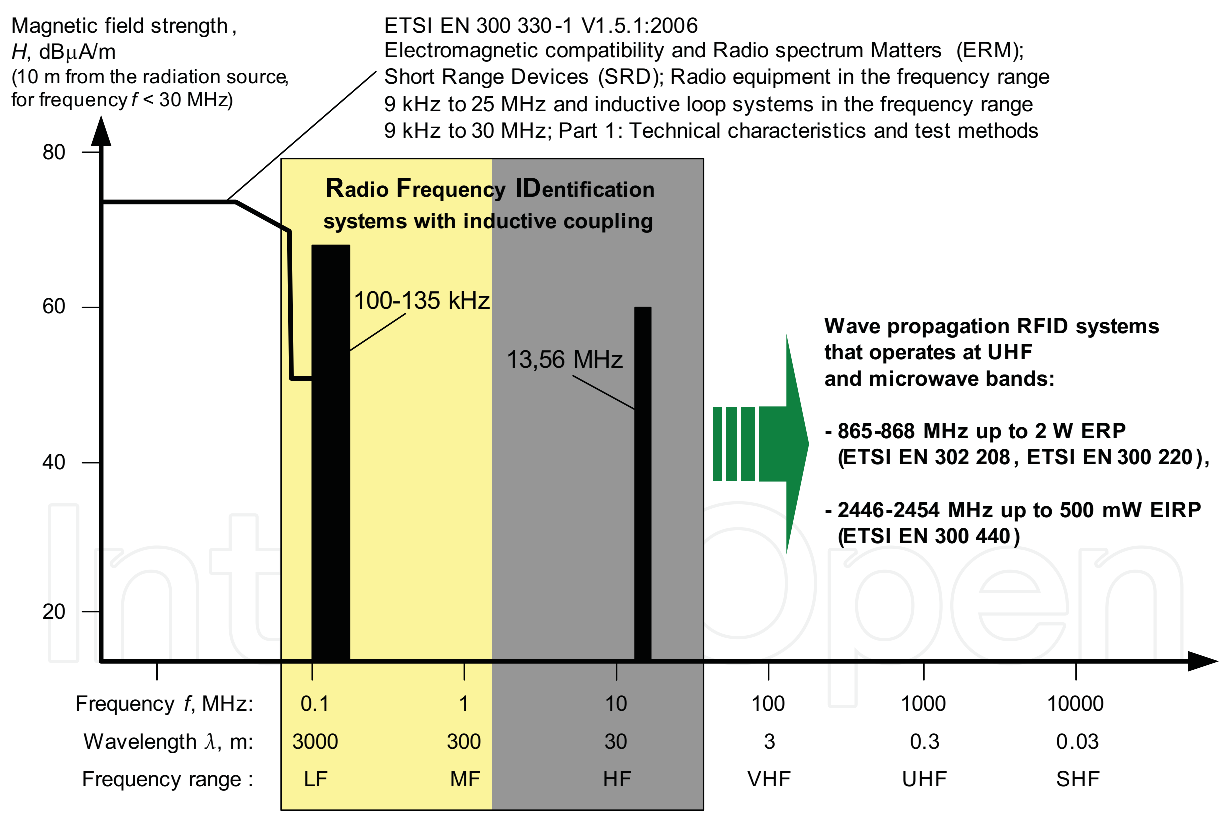

Fig. 2. Frequency ranges and European licensing regulation for RFID systems

Frequency bands widely available for different kind of radio systems (called ISM - Industrial-Scientific-Medical) are used in contact-less identification of objects (ERC, 2008). Therefore, it is required to reduce the magnetic field strength produced by a transmitting antenna of low frequency systems, and reduce the effective radiated power for systems operating in the range of ultra-short waves and microwaves.

Contact-less inductively coupled systems are used to identify objects in the range of the lowest frequencies (in the wave ranges from medium to short). These systems are currently the most widespread, developed and supported by all the key suppliers of RFID components (Yan et al., 2008). They are characterized by working in the area where a strong magnetic coupling between antennas of transmitting components occurs and also where there is strong wave mismatching between communication equipments (Flores et al., 2005). Assuming that the wave propagates in a vacuum, the phase coefficient β takes the real value:

$$\beta = \omega\sqrt{\mu_0 \varepsilon_0} \tag{1}$$

where ω denotes the pulsation, μ_0 – magnetic permeability of vacuum whereas ε_0 means electric permittivity of vacuum.
With respect to the classical theory of antennas, it is possible to specify the working distance of inductively coupled RFID systems according to the following conditions (Fig. 3):

- for an induction zone - near field (all systems with inductive coupling):

$$z << \lambda \tag{2}$$

- for a Fresnel zone (systems operating in the range of short-wave):

$$\beta \cdot z > 1 \tag{3}$$

with signs appearing in the dependencies (2) and (3) described in Fig. 3.

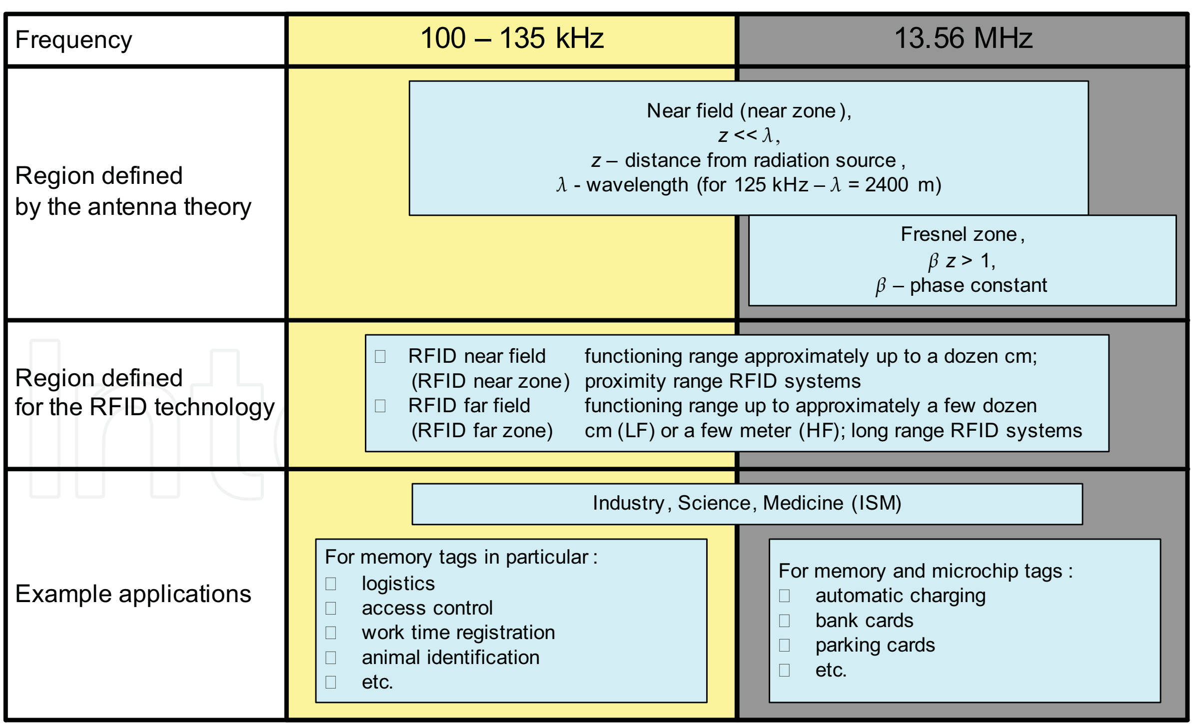

Fig. 3. Operating region of RFID systems with inductive coupling

The average distance between the transmitter and the receiver is from a few centimetres to several meters in the case of RFID systems operating in the range of short-wave. For such a separated working area, the value of the energy flux density transmitted by an electromagnetic wave (Poynting vector) is zero. This means that the functional principle of RFID systems with inductive coupling is primarily storage of energy in the magnetic field. Examples of working distances, detailed specified ranges and operating limit of two inductively coupled RFID systems are shown in Fig. 4.

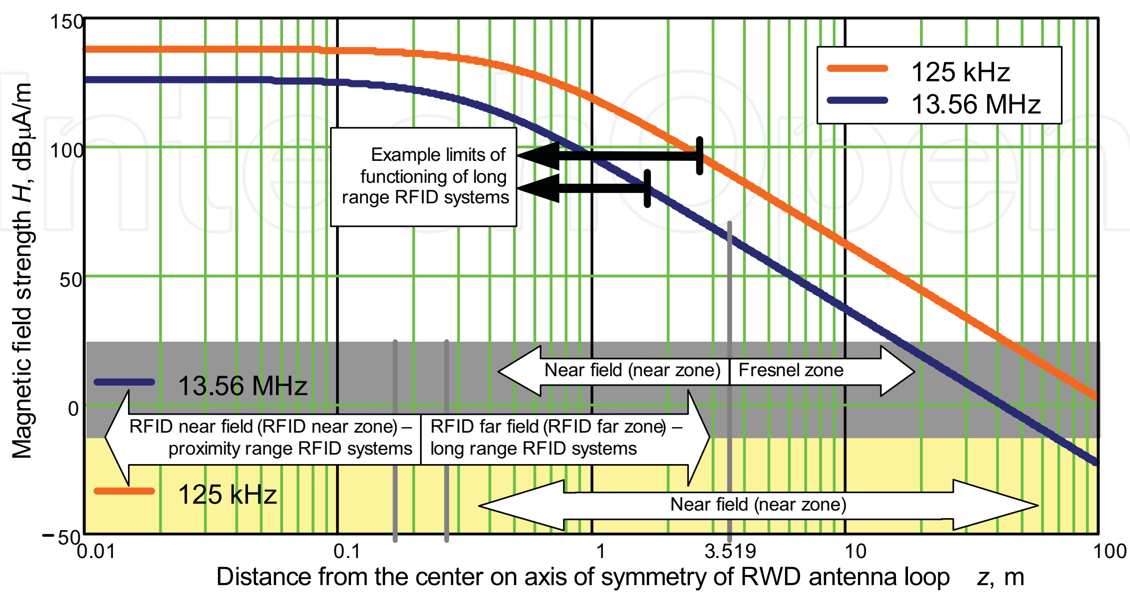

Fig. 4. Magnetic field strength for the transmitting antennas operating at the frequency of 125 kHz and 13.56 MHz with a specification of the working scope according to the classical theory of antennas and for RFID systems with inductive coupling.

With regard to the established characteristic of working distance in RFID systems, the two working scopes are defined. The RFID near field which means the operating distance up to about a dozen centimetres and the RFID far field where the operating range is around from few dozen centimetres to several meters (Bhatt & Glover, 2006; Finkenzeller, 2003; Paret, 2005). It should be noted that these limits, for both the classical theory of antennas as well as RFID systems, are not distances at which rapid changes in transmission parameters occur. Both the changes in properties of the electromagnetic field (zero or nonzero value of the Poynting vector) as well as changes in the efficiency of interaction between communication equipments (which differ in structures depending on a range for RFID near-and far field) have continuous character at estimated boundaries.

3. Restrictions on the magnetic field strength in RFID systems with inductive coupling

The issue of radio system operation is connected with electromagnetic radiation. With regard to the operation correctness and proper construction of RFID system it is necessary to recognise harmful effects of electromagnetic field on the human body and to determine acceptable radiation standards (EN 50364, 2001; EN 50357, 2001; IEC 62369, 2008). In the field of RFID systems with inductive coupling the restrictions of the magnetic field strength are contained in ETSI EN 300 330 standard (ETSI, 2006), which is based on CEPT/ERC Recommendation 70-03 document (ERC, 2008). This document was prepared by the European Telecommunications Standards Institute whose goal is to define standards in the broad area of telecommunications systems.

Class	Device description	Antenna area S	Length of antenna	Description
1	Inductive loop coil transmitter	< 30 m^2	< $\lambda/4$ or < 75 m / f where: λ – wavelength f – frequency in MHz	Integrated antenna with a transmitter or directly connected with it
2	Inductive loop coil transmitter	< 30 m^2	< $\lambda/4$ or < 75 m / f	Designed antenna with attached instructions
3	Customized large size loop antennas only	> 30 m^2	-	-
4	E-field transmitter	-	-	-

Table 1. Description of classes of transmitting device in accordance to ETSI EN 300 330

In the Part 1*: Technical characteristics and test methods of the ETSI EN 300 330: Electromagnetic compatibility and Radio spectrum Matters (ERM); Short Range Devices (SRD); Radio equipment in the frequency range 9 kHz to 25 MHz and inductive loop systems in the frequency range 9 kHz to 30 MHz*, are defined four classes of transmitting devices, which are summarized in Table 1. Due to the fact that all of RFID systems with inductive coupling operating in the frequency range 9 kHz to 30 MHz belong to Class 1 and 2, the restrictions of the magnetic field strength are compared in Table 2 only for those classes of transmitting devices.

Nr.	Frequency f, MHz	Magnetic field strength limits at 10 m H_{10max}, dBμA/m
1	$0.009 \le f < 0.315$	30
2	$0.009 \le f < 0.03$	72
3	$0.03 \le f < 0.05975$ $0.06025 \le f < 0.07$ $0.119 \le f < 0.135$	72 at 0,03 MHz descending 3 dB/oct
4	$0.05975 \le f < 0.06025$ $0.07 \le f < 0.119$ $0.135 \le f < 0.140$	42
5	$0.140 \le f < 0.1485$	37.7
6	$0.1485 \le f < 30$	-5
	$0.315 \le f < 0.600$	-5
7	$3.155 \le f < 3.400$	13,5
8	$7.400 \le f < 8.800$	9
9	$10.20 \le f < 11.00$	9
10	$6.765 \le f < 6.795$ $13.553 \le f < 13.567$ $26.957 \le f < 27.283$	42
11	$13.553 \le f < 13.567$	60

Table 2. Magnetic field strength limits at 10 m from radiation source

The restrictions listed in items 2 and 3 of Table 2 for the frequency bands 9-10 kHz and 119-135 kHz are valid for loop antennas with an area of $S \geq 0.16$ m². If the antenna surface of the transmitting devices is in the range from 0.05 m² to 0.16 m², the limit value of H_{10max} has to be corrected according to the following relationships:

$$H_{10max,cor} = H_{10max} + 10\log\left(\frac{S}{0{,}16m^2}\right) \quad (4)$$

It is necessary to reduce the limit values given in Table 2 by 10 dB for loop antennas with an area of S <0.05 m².

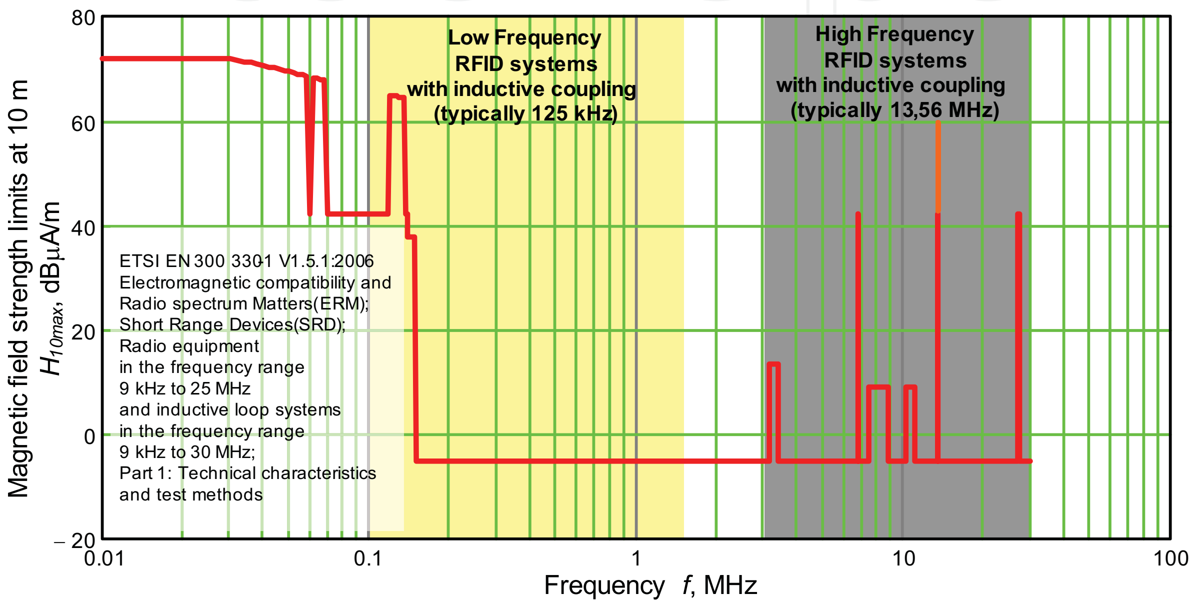

(a)

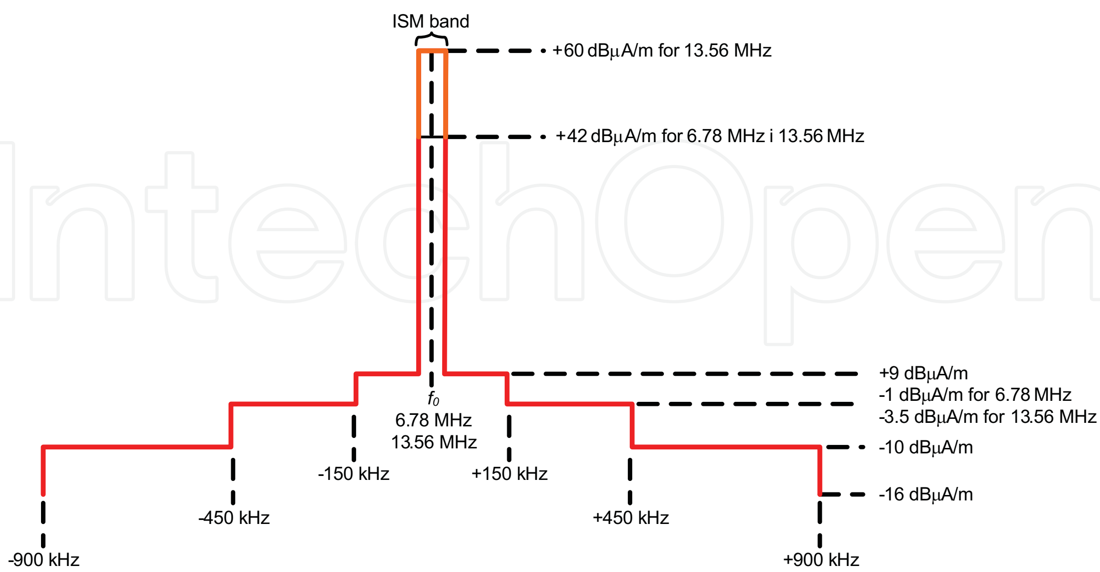

(b)

Fig. 5. Magnetic field strength limits at 10 m from radiation source: a) frequency range 0.01 MHz – 30 MHz, b) spectrum mask limit for frequency: 6.78 MHz and 13.56 MHz

A graphical representation of the magnetic field strength limit specified in Table 2 is shown in the Fig. 5-a. Apparent increase in this curve from 42 dBµA/m to 60 dBµA/m in the range including an operating frequency of 13.56 MHz applies only to systems with inductive coupling, and also to electronic supervision systems called *Electronic Article Surveillance* (EAS). In this case, detailed representation of the magnetic field strength limit reflects a mask which defines the reduction of the limit value H_{10max} in the band ± 900 kHz of working frequency 13.56 MHz (Fig. 5-b).

In most cases, as was already mentioned communication between the transmitter and receiver in inductively coupled RFID systems takes place at a maximum distance of several meters. For this reason, it is useless to define magnetic field strength limit at the distance of 10 m from the radiation source. In order to fulfil the requirements of radiation standards with regard to designing of antenna units the maximum magnetic field strength is determined at a distance of 3 meters from the antenna, according to the relationship:

$$H_{3max} = H_{10max} + C_3 \tag{5}$$

where C3 is a correction factor (expressed in dB) described by a curve which is shown in the Fig. 6.

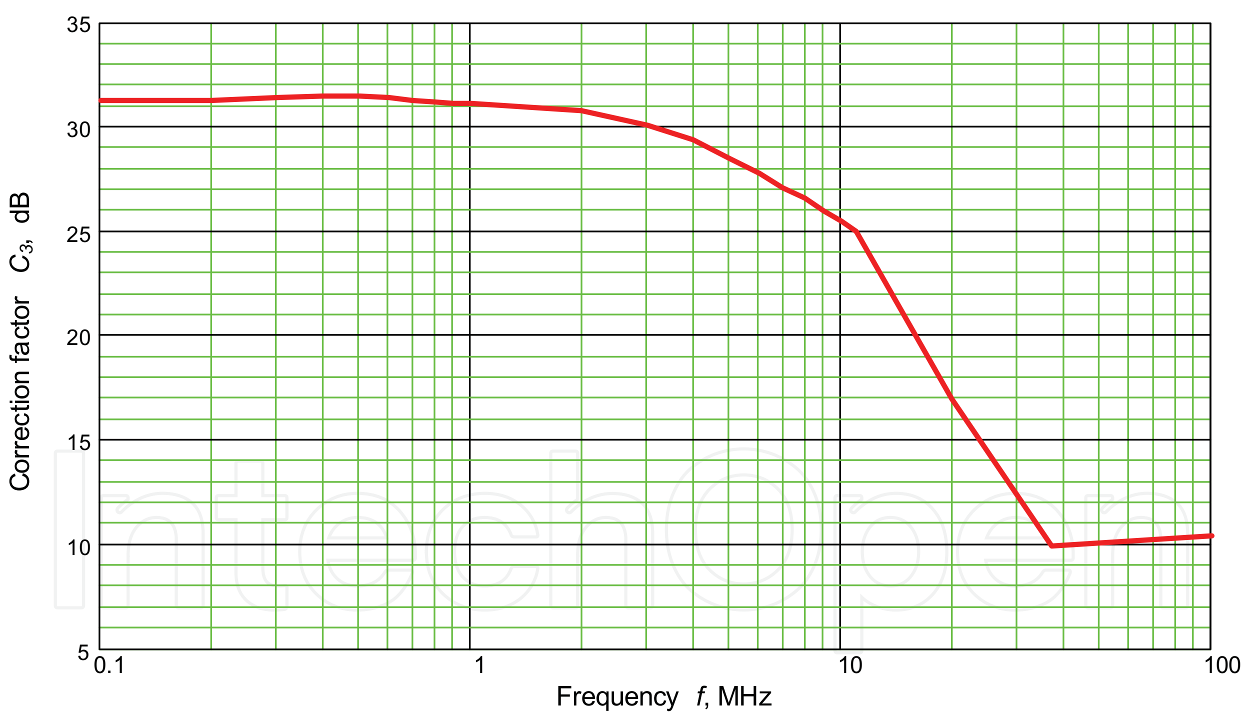

Fig. 6. Correction factor C_3 versus frequency, for limits of magnetic field strength at the distance of 3 m from radiation source

Paying attention to the maximum working distance between elements of the RFID system, in particular for systems working in the RFID far field, it is necessary to estimate the simulated and built antenna set RWD-tags in relation to the obligatory normalizations in communication systems and Electro-Magnetic Compatibility (EMC).

4. Energy transfer in RFID system with inductive coupling

4.1 Magnetic induction value around RWD antenna loop

Analysis of the Read/Write Device (RWD) antenna unit in the area of RFID systems with inductive coupling, permits to make an assumption, that the antenna loop current (I_R) is constant along the whole flow way. This means that the current intensity is constant for any part of the loop which forms an RWD antenna. Fluctuation in the electric charge density equals zero in given period of time, so in that case the divergence of electric current density **J** equals zero as well:

$$\nabla \cdot \mathbf{J} = 0 \tag{6}$$

Making the above mentioned assumptions allows to apply the magnetostatic laws to magnetic field analysis for any shape of RWD antenna loops.

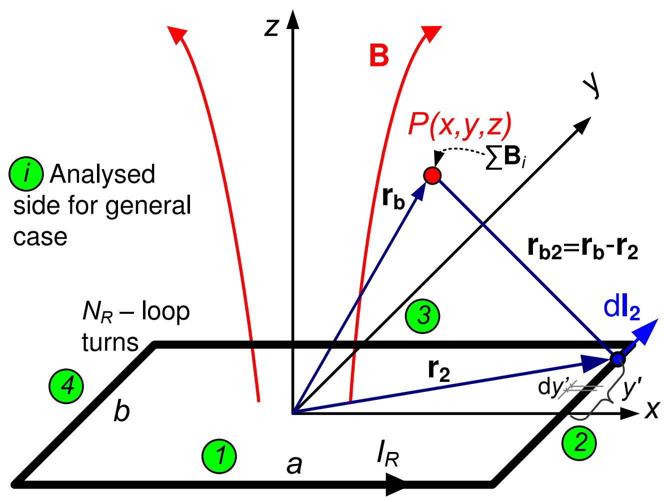

Fig. 7. Analyzed case of polygon shape of RWD antenna loop

In the case of RWD antenna loop constructed as polygon (Fig. 7), Biot-Savart law with superposition theorem (Halliday et al., 2004) permits to sum vectors of magnetic induction **B** that descend from individual antenna parts at location $P(x,y,z)$. In this case the total magnetic induction is calculated from equation:

$$\mathbf{B} = \sum_i \mathbf{B}_i \tag{7}$$

where i denotes analysed side for RWD antenna loop constructed as polygon.
The vectors $\mathbf{r}_{bi}$ describing the $d\mathbf{l}_i$ (for i=1, 2, 3, 4) location at P point, in which the value of magnetic induction is calculated, are given by formulas:

$$\mathbf{r}_{b1} = \mathbf{r}_b - \mathbf{r}_1 , \tag{8}$$

$$\mathbf{r}_{b2} = \mathbf{r}_b - \mathbf{r}_2 , \tag{9}$$

$$\mathbf{r}_{b3} = \mathbf{r}_b - \mathbf{r}_3 , \tag{10}$$

$$\mathbf{r}_{b4} = \mathbf{r}_b - \mathbf{r}_4 \tag{11}$$

where the vectors describing $\mathbf{dl_i}$ elements location, and the vector $\mathbf{r_b}$ describing location of point *P*, are given as follows:

$$\mathbf{r}_1 = \begin{pmatrix} x' \\ -b/2 \\ 0 \end{pmatrix}, \tag{12}$$

$$\mathbf{r}_2 = \begin{pmatrix} a/2 \\ y' \\ 0 \end{pmatrix} \tag{13}$$

$$\mathbf{r}_3 = \begin{pmatrix} x' \\ b/2 \\ 0 \end{pmatrix}, \tag{14}$$

$$\mathbf{r}_4 = \begin{pmatrix} -a/2 \\ y' \\ 0 \end{pmatrix}, \tag{15}$$

$$\mathbf{r}_\mathbf{b} = \begin{pmatrix} x \\ y \\ z \end{pmatrix} \tag{16}$$

The unit vectors $\mathbf{u_1}$-$\mathbf{u_4}$ connected with $\mathrm{d}\mathbf{l}_{1,3} = \mathbf{u}_{1,3} \cdot \mathrm{d}x'$ and $\mathrm{d}\mathbf{l}_{2,4} = \mathbf{u}_{2,4} \cdot \mathrm{d}y'$ are given by formulas:

$$\mathbf{u}_1 = \mathbf{u}_3 = \begin{pmatrix} 1 \\ 0 \\ 0 \end{pmatrix}, \tag{17}$$

$$\mathbf{u}_2 = \mathbf{u}_4 = \begin{pmatrix} 0 \\ 1 \\ 0 \end{pmatrix} \tag{18}$$

After the $\mathbf{B}_i$ calculated for analysed side of RWD antenna loop, on the basis of (7), the magnetic vector at any space location with (*x,y,z*) coordinates is given as follows:

$$\mathbf{B} = \frac{\mu_0 I_R N_R}{4\pi} \left[\int_{\frac{-a}{2}}^{\frac{a}{2}} \frac{\mathbf{u_1} \times \mathbf{r_{b1}}}{\left|\mathbf{r_{b1}}\right|^3} \mathrm{d}x' + \int_{\frac{-b}{2}}^{\frac{b}{2}} \frac{\mathbf{u_2} \times \mathbf{r_{b2}}}{\left|\mathbf{r_{b2}}\right|^3} \mathrm{d}y' + \int_{\frac{a}{2}}^{\frac{-a}{2}} \frac{\mathbf{u_3} \times \mathbf{r_{b3}}}{\left|\mathbf{r_{b3}}\right|^3} \mathrm{d}x' + \int_{\frac{b}{2}}^{\frac{-b}{2}} \frac{\mathbf{u_4} \times \mathbf{r_{b4}}}{\left|\mathbf{r_{b4}}\right|^3} \mathrm{d}y' \right] \tag{19}$$

where: $\mu_0 = 4 \cdot \pi \cdot 10^{-7}$ H/m.
The components of magnetic induction *B* in any space point *P(x,y,z)* are given for polygon shape of RWD antenna loop by equations:

$$B_x = \frac{\mu_0 I_R N_R}{4\pi}\left[\int_{\frac{-b}{2}}^{\frac{b}{2}} \frac{z}{\left[\left(x-\frac{1}{2}a\right)^2+\left(y-y'\right)^2+z^2\right]^{3/2}}\mathrm{d}y' + \int_{\frac{b}{2}}^{\frac{-b}{2}} \frac{z}{\left[\left(x+\frac{1}{2}a\right)^2+\left(y-y'\right)^2+z^2\right]^{3/2}}\mathrm{d}y'\right] \quad (20)$$

$$B_y = \frac{\mu_0 I_R N_R}{4\pi}\left[\int_{\frac{-a}{2}}^{\frac{a}{2}} \frac{-z}{\left[\left(x-x'\right)^2+\left(y+\frac{1}{2}b\right)^2+z^2\right]^{3/2}}\mathrm{d}x' + \int_{\frac{a}{2}}^{\frac{-a}{2}} \frac{-z}{\left[\left(x-x'\right)^2+\left(y-\frac{1}{2}b\right)^2+z^2\right]^{3/2}}\mathrm{d}x'\right] \quad (21)$$

$$B_z = \frac{\mu_0 I_R N_R}{4\pi}\cdot\left[\int_{\frac{-a}{2}}^{\frac{a}{2}} \frac{y+\frac{1}{2}b}{\left[\left(x-x'\right)^2+\left(y+\frac{1}{2}b\right)^2+z^2\right]^{3/2}}\mathrm{d}x' + \int_{\frac{-b}{2}}^{\frac{b}{2}} \frac{-x+\frac{1}{2}a}{\left[\left(x-\frac{1}{2}a\right)^2+\left(y-y'\right)^2+z^2\right]^{3/2}}\mathrm{d}y' + \right.$$
$$\left. + \int_{\frac{a}{2}}^{\frac{-a}{2}} \frac{y-\frac{1}{2}b}{\left[\left(x-x'\right)^2+\left(y-\frac{1}{2}b\right)^2+z^2\right]^{3/2}}\mathrm{d}x' + \int_{\frac{b}{2}}^{\frac{-b}{2}} \frac{-x-\frac{1}{2}a}{\left[\left(x+\frac{1}{2}a\right)^2+\left(y-y'\right)^2+z^2\right]^{3/2}}\mathrm{d}y'\right] \quad (22)$$

The obtained equations (20)-(22) permit numerical calculation of magnetic induction value separately for individual components in directions x, y and z (B_x, B_y, B_z). These equations enable to evaluate direction and sense of magnetic induction vector. The example of MathCad 14 calculation for polygon shape of RWD antenna loop, which parameters are given by: a=0.3 m, I_R=0.2 A, has been presented in Fig. 8.

The variable value of z component of magnetic induction (B_z) (which has been presented as an example) reveals the problem of the correct localization of the tag in the space what is necessary in order to fulfill the condition of minimum value of induction (B_{min}). In turn, the alternating direction of the normalized magnetic induction vector (B_{norm}) indicates the problem of correct orientation for tag in relation to individual components of this vector. For example, the correction of tag orientation can occur in order to ensure its maximum distance from the RWD antenna. It can also be forced by the characteristic of the objects that are identified, namely it means the need to locate a tag on the labeled object in a special way (e.g. in bevel boxes placed on a pallet exposed to a process of anticollision identification). In many cases, the anticipated specification of tags localization in practical applications (for transponders working first of all in anticollision but also in single RFID systems) indicates the necessity of considering induction component in the direction of z axis. However, for correct estimation of the performance efficiency for the real RFID system in the field conditions area it is required to determine the tag orientation influence on the correct identification (Jankowski-M. et al., 2008).

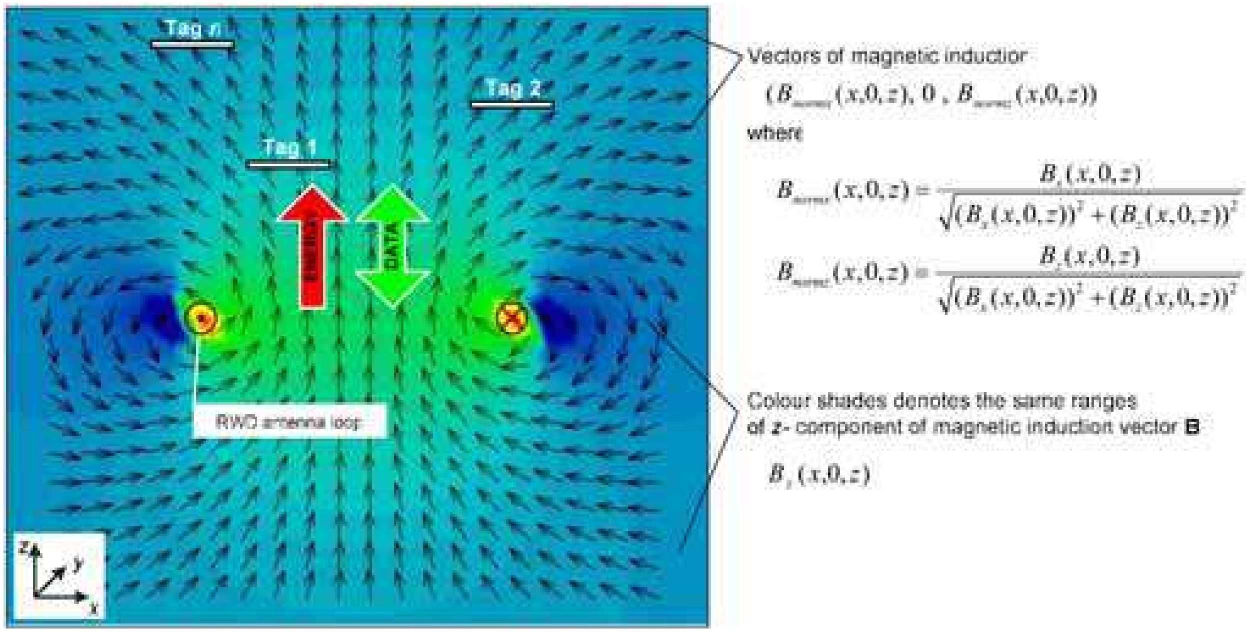

Fig. 8. Magnetic induction in *x*-z plane and tags localization in magnetic field of RWD antenna loop

4.2 Tag orientation in magnetic field of RWD antenna loop

A lot of practical solutions of identification are characterized by parallel location of tag antenna and RWD loop. This location of individual tags allows the magnetic induction B_{min} to reach its minimum value only in relation to *z*-magnetic induction components. This case applies to places, in which tags working in anticollision process has been located ($P_1(x_1,y_1,z_1) \div P_n(x_n,y_n,z_n)$ – Fig. 1). Presented approach creates a lot of limits connected with decrease of the interrogation zone in RFID system. This results from too low value of the **perpendicular magnetic induction component** in relation to tag antenna loop plane.

The efficient use of communication space, in which anticollision process is going to be done, and also specification of the object marked by passive RFID tag, requires consideration of any tag orientation with regard to the individual components of magnetic induction vector (Fig. 9).

The issue of any tag orientation in three dimensions *x-y-z* comes down to tag deviation by α and β angles from parallel location of RWD-tag antenna loops (Fig. 9-a). In accordance with presented model (Fig. 9-b and Fig. 9-c), deviation by α angle occurs in *z-x* plane, however deviation by β angle occurs in α-*y* plane. The value calculation of perpendicular magnetic induction component for tag, which is deviated by α and β angles ($B_{\alpha\beta}$), has been divided in two parts. In the first part, by using superposition theorem, after deviating tag by α angle, the perpendicular magnetic induction component is given by:

$$B_{xz\alpha} = B_{x\alpha} + B_{z\alpha} \tag{23}$$

where the values of vector components are given by:

$$B_{x\alpha} = B_x \cdot \sin(\alpha)\,, \tag{24}$$

$$B_{z\alpha} = B_z \cdot \cos(\alpha) \tag{25}$$

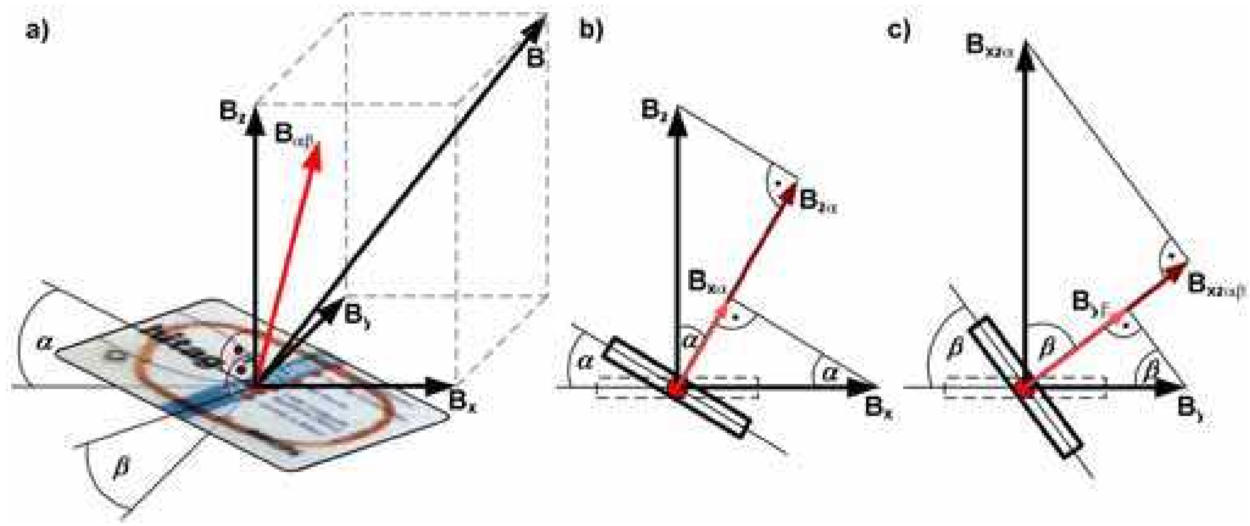

Fig. 9. Orientation of tag, which is deviated by α and β angles from components of magnetic induction vector: a) deviation in 3D coordinate *x-y-z*; b) deviation by α angle in *z-x* plane; c) deviation by β angle in α-*y* plane

Next, in second part, by using of the superposition theorem, after deviating tag by β angle, the perpendicular magnetic induction component is given as follows:

$$B_{\alpha\beta} = B_{y\beta} + B_{xz\alpha\beta} \tag{26}$$

where the values of vector components are given by:

$$B_{y\beta} = B_y \cdot \sin(\beta)\,, \tag{27}$$

$$B_{xz\alpha\beta} = B_{xz\alpha} \cdot \cos(\beta) \tag{28}$$

It comes from the equations (23)-(28) that the perpendicular magnetic induction component for passive tag which is deviated by α and β angles is given by:

$$B_{\alpha\beta} = B_z \cdot \cos(\alpha) \cdot \cos(\beta) + B_x \cdot \sin(\alpha) \cdot \cos(\beta) + B_y \cdot \sin(\beta) \tag{29}$$

Knowing the magnetic induction separately for individual components in directions *x*, *y* and *z* (B_x, B_y, B_z), the obtained equation (29) permits calculation of the perpendicular magnetic induction component. The aforementioned necessity of changing tag orientation should be carried out for assurance of correct tag work in the individual space point *P(x,y,z)*. In this way, there is possible to calculate the system interrogation zone which is forced by specification of identified object what results from the necessity of individual tag location on marked object.

Changes of the interrogation zone for single tag with minimal value of magnetic induction have been presented as examples in Fig. 10-c, d (calculated results) and Fig. 10-b (measured results). The black colour represents **no communication area** between tag and RWD. The area results from no fulfil condition of minimal magnetic induction (B_{min}) for the tag and its location in relation to perpendicular magnetic induction component.

Above mentioned parallel location of tag and RWD antenna loops causes appearance of symmetrical interrogation zone and lack of communication area in relation to symmetry axis

of RWD antenna (Fig. 10-c). The both areas on *x-y* plane have been presented in upper part of diagram. Any changes in tag orientation by α and β angles (Fig. 10-b, d) lead to modifications in the interrogation zone. For the given tag and its hypothetical orientation, the communication area has been significantly shifted in direction of tag deviation, while no communication areas between tag and RWD has appeared in the central part of *x-y* plane.
The axial symmetry of interrogation zone and no-communication zone disappears in case of tag deviation by α and β angles. Such state complicates forecast and unambiguous description of the tag location, which permits its correct work.

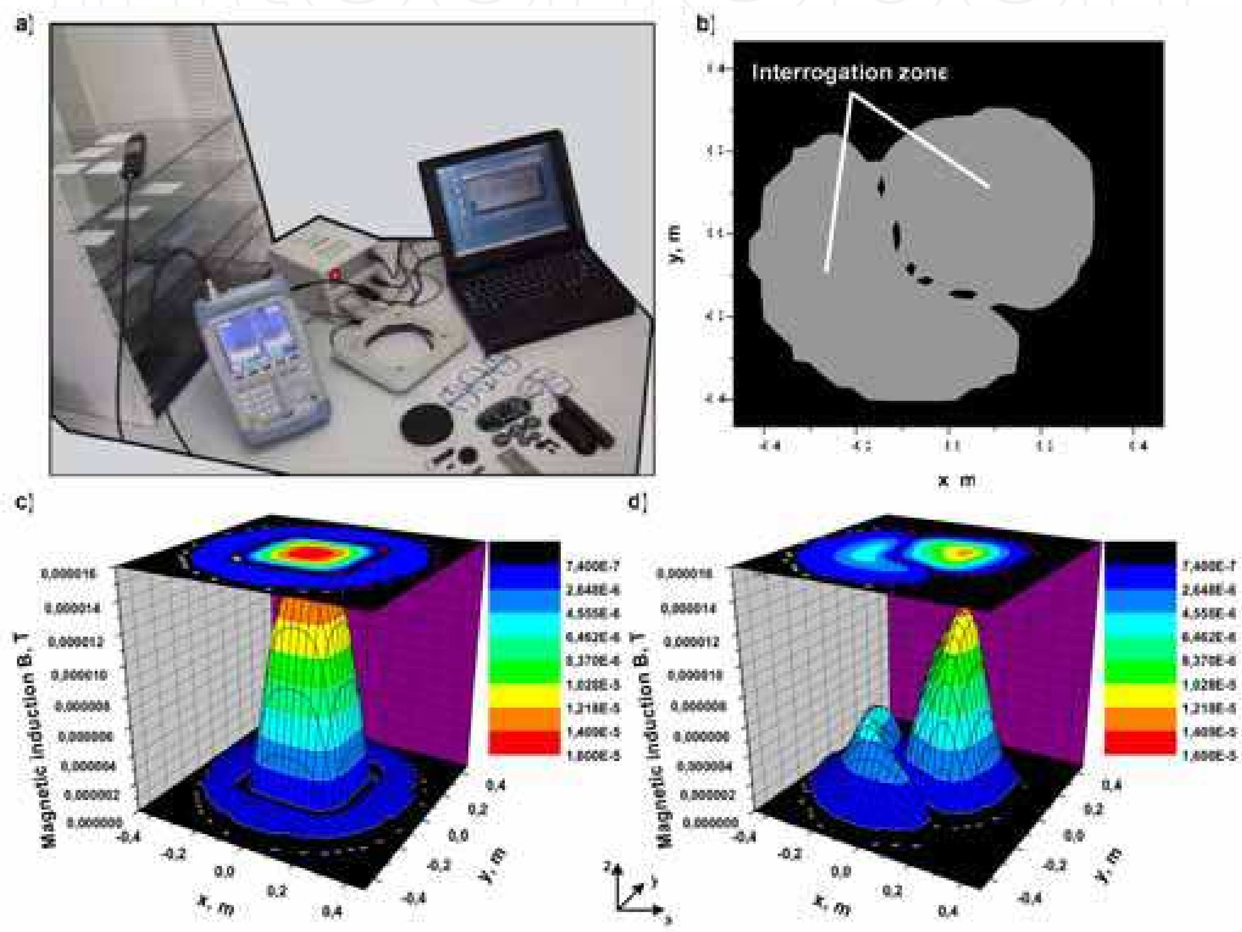

Fig. 10. Perpendicular magnetic induction component for HITAG 1 ISO CARD (B_{min}=740 nT) placed in 0.1m distance from square RWD antenna (*a* side = 0.3 m):
a) laboratory system, b) measured interrogation zone for deviated tag by α, β=45º,
c) calculated result - α, β=0º; d) calculated result - deviated tag by α, β=45º

In case of required passive tag deviation from symmetry axis of antenna loops, the value of perpendicular magnetic induction component should be always corrected according to the equation (29), which takes into consideration tag deviation by α and β angles. During the analysis of field conditions, the effect of RWD antenna shape on communication should be considered additionally. Calculation of the above parameters for given single and anticollision 3D identification system gives the basis to determine the interrogation zone of passive RFID systems.

4.3 Structural conditions of RWD antenna loop

In the literature on the subject, the magnetic induction relationship for circular conductor with current is often applied (Cichos, 2002; Microchip, 2004). A situation, when tag antenna loop is placed on axis of symmetry with RWD antenna loop, is the characteristic case of radio frequency identification system functioning. The estimation of circle radius on the basis of the real RWD loop area which is a polygon can lead to errors during the calculation of maximum working distance for RFID system. The shape of RWD antenna influences on location of magnetic lines in 3D space, therefore the relationships for different shape of read/write device antenna loop have been presented in Table 3. They are derived from the Biot-Savart law in accordance with the described method, which permits to analyze any shape of RWD antenna loop required by system designer (Jankowski-M. & Kalita, 2004).

Nr.	RWD antenna shape	Magnetic induction ***B*** in distance ***z*** from the center on axis of symmetry of RWD antenna loop
1	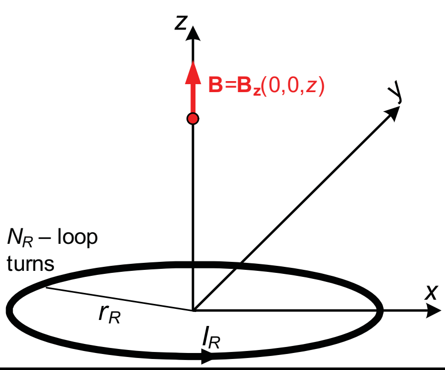	$B = \frac{\mu_0 I_R N_R r_R^2}{2\left(z^2 + r_R^2\right)^{3/2}}$
2	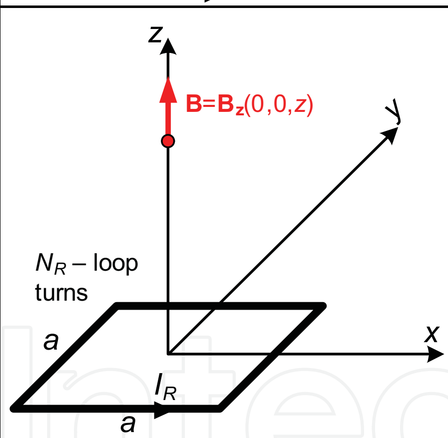	$B = \frac{4\mu_0 I_R N_R a^2}{\pi\left(4z^2 + a^2\right)\left(4z^2 + 2a^2\right)^{1/2}}$
3	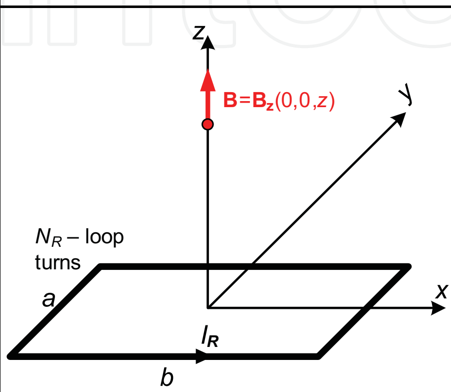	$B = \frac{2\mu_0 I_R N_R}{\pi}\left[\frac{a^2}{\left(4z^2 + a^2\right)\left(4z^2 + 2a^2\right)^{1/2}} + \frac{b^2}{\left(4z^2 + b^2\right)\left(4z^2 + 2b^2\right)^{1/2}}\right]$

Table 3. Magnetic induction value for different shape of RWD antenna loop

For the sake of the fact that the shape of RWD loop determines the magnetic field, there has been presented below the method of calculating the magnetic induction B created on the square coil consisted of N_R loop turns, each through the current I_R is flowing. Considerations concern z axis, because RFID systems are projected in such way, that the tag antenna loop is situated on one of axis of symmetry with RWD loop.
In accordance with Biot-Savart law, the d**B** value is given by equation:

$$d\mathbf{B} = \frac{\mu_0 I_R N_R}{4\pi} \cdot \frac{d\mathbf{l}\sin(\theta)}{r^2} \tag{30}$$

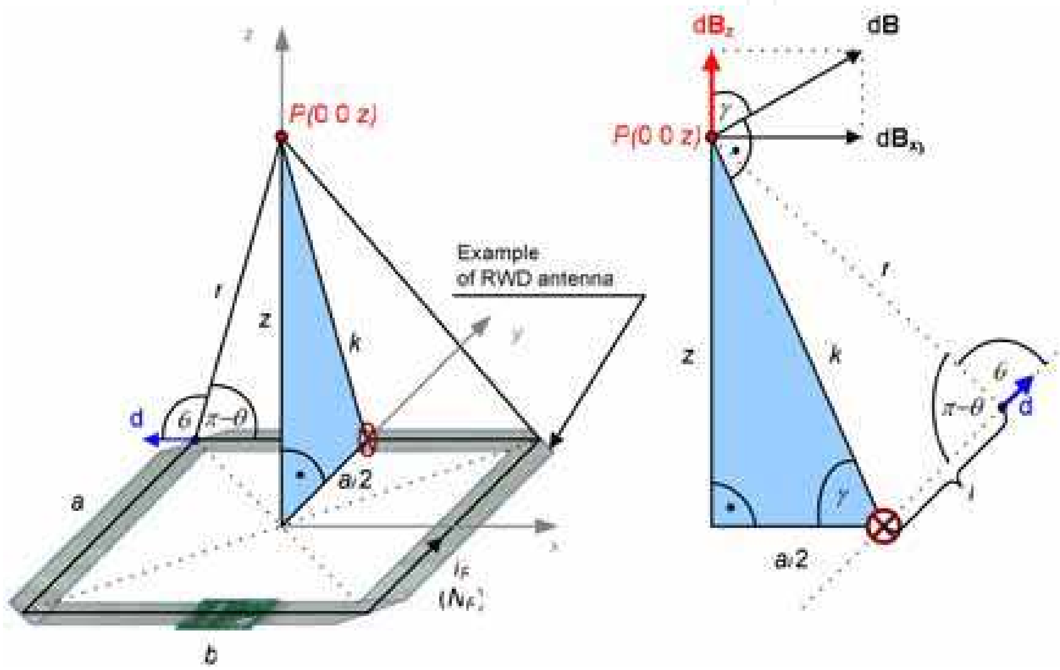

Fig. 11. Analyzed case of polygon shape of RWD antenna loop

Spreading d**B** on two components: d$\mathbf{B}_{xy}$ - perpendicular to z axis and d$\mathbf{B}_z$ - parallel to z axis, there can be noticed, that at location $P(0,0,z)$ only the d$\mathbf{B}_z$ has an influence on magnetic induction **B** vector. Such state result from the fact, that the sum of d$\mathbf{B}_{xy}$ components, with reference to whole current currying conductor - equals 0 for the sake of symmetry. In that case:

$$\mathbf{B} = \int d\mathbf{B}_z \tag{31}$$

where:

$$d\mathbf{B}_z = d\mathbf{B}\cos(\gamma) \tag{32}$$

Defining the geometrical relationships between the individual angles and sides at location P, placed in x distance, they can be rewritten:

$$\sin(\theta) = \sin(\pi - \theta) = \frac{k}{r}, \tag{33}$$

$$r = \sqrt{k^2 + l^2}\ , \tag{34}$$

$$k = \sqrt{z^2 + \left(\frac{a}{2}\right)^2}\ , \tag{35}$$

$$\cos(\gamma) = \frac{a}{2k} \tag{36}$$

Substituting suitably (30) and (33)-(36) to (32) equation, and then whole to (31) equation, there can be received:

$$B = \int \mathrm{d}B_z = \int \mathrm{d}B \cdot \cos(\gamma) = 2 \cdot \frac{\mu_0 I_R N_R}{4\pi}\left[\int_{-\frac{a}{2}}^{+\frac{a}{2}} \frac{\frac{a}{2}}{\left(z^2 + \left(\frac{a}{2}\right)^2 + l^2\right)^{3/2}}\mathrm{d}l + \int_{-\frac{b}{2}}^{+\frac{b}{2}} \frac{\frac{b}{2}}{\left(z^2 + \left(\frac{b}{2}\right)^2 + l^2\right)^{3/2}}\mathrm{d}l\right] \tag{37}$$

In result of the (37) integration, the (38) equation can be obtained. It allows to estimate the value of magnetic induction B in distance z from the centre on symmetry axis of square RWD antenna loop:

$$B = \frac{2\mu_0 I_R N_R}{\pi}\left[\frac{a^2}{\left(4z^2 + a^2\right)\left(4z^2 + 2a^2\right)^{1/2}} + \frac{b^2}{\left(4z^2 + b^2\right)\left(4z^2 + 2b^2\right)^{1/2}}\right] \tag{38}$$

In the Fig.12, there are presented the curves $B=f(z)$ for the RWD antenna loops with equal areas but different shapes: (1) - circular, (2) - square and (3, 4, 5, 6) - rectangle, where the ratio of the sides a/b is given as follows: 0.028, 0.111, 0.25, 0.44. The line B_{min} (for analyzed tag) intersects the curve of value of the magnetic induction for analyzed shape of RWD antenna loop, what leads to evaluation of the maximum working distance z_{max} of RFID system.

The equation number 1 from table 3 is valid only for a case of circular and square shape of RWD antenna loop. In the case of rectangle RWD antenna (or a loop which is constructed as other polygon) where $a/b < 1$, there is irregularity in calculation of the maximum working distance of RFID system (Fig. 12). If the coefficient $a/b \ll 1$ or when RWD antenna is constructed as a complicated polygon, the error may be significant and as a consequence may lead to wrong result in estimation process of interrogation zone which was assumed at first. The interrogation zone of RFID system for two extreme cases from Fig. 12 has been presented in Fig. 13.

Depending on required uses (the identification of animals, access control or objects identification in logistics), the process of calculating the maximum working distance should take into consideration the fallowing aspects: the real shape of RWD antenna, three-dimensional location of tag, its orientation and kind of executed operation - writing or reading data from internal tag memory (Jankowski-M. & Kalita, 2004).

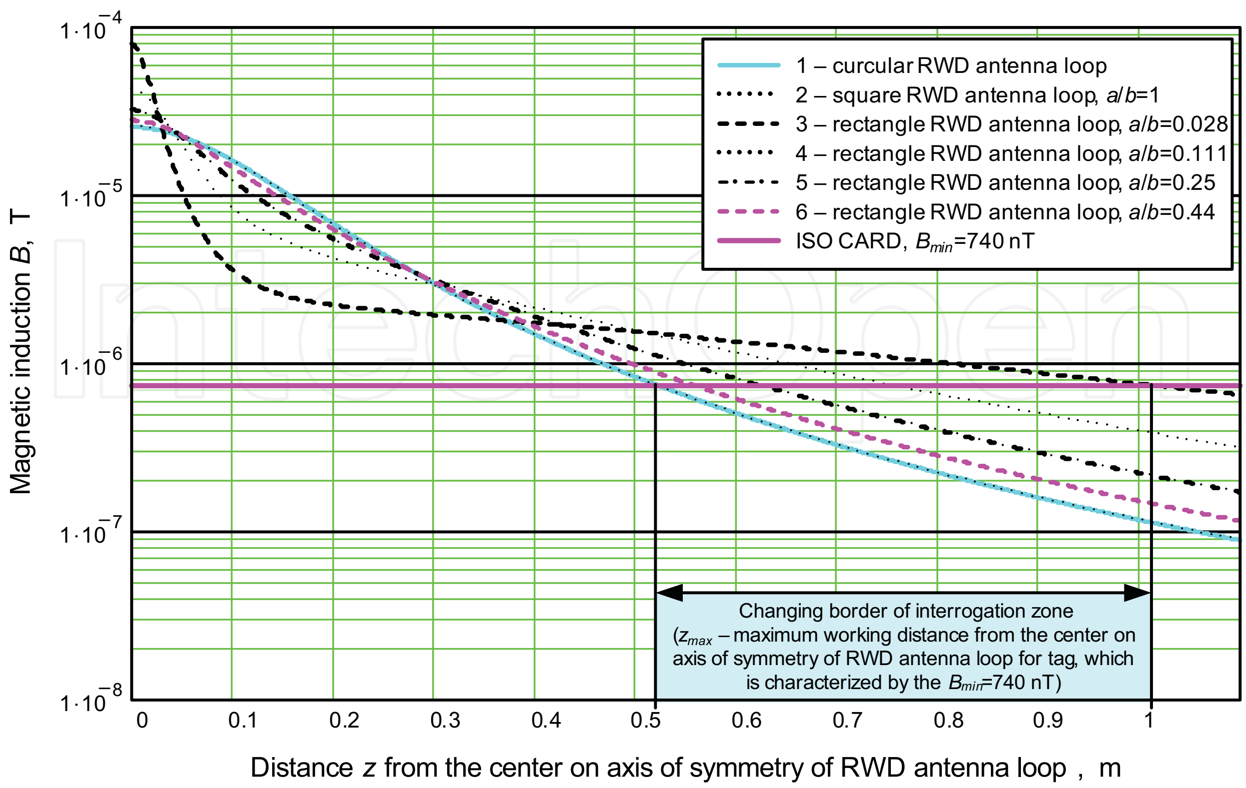

Fig. 12. Curves of value of the magnetic induction in function of distance z from the center on axis of symmetry of RWD antenna loop with equal areas

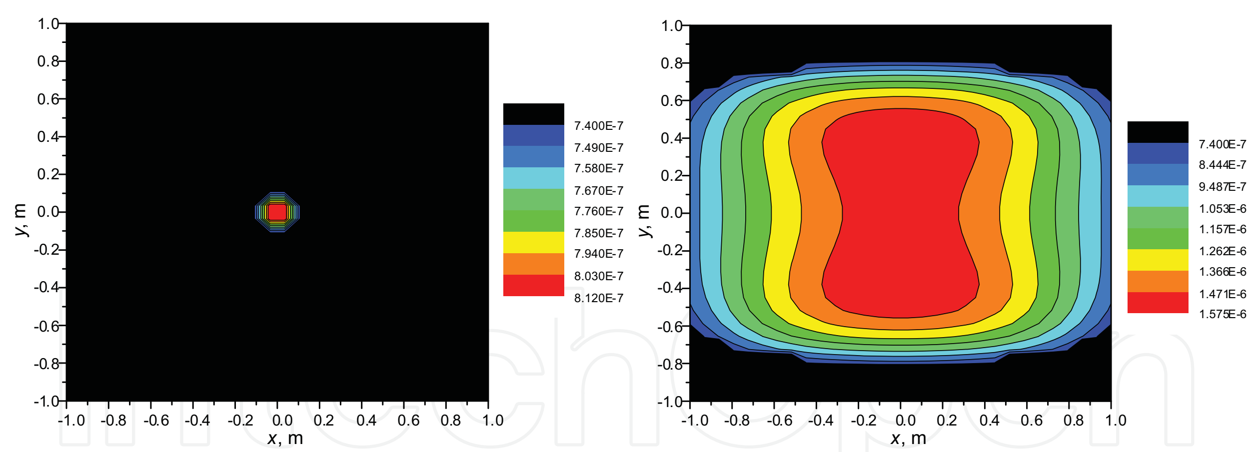

(a) (b)

Fig. 13. Perpendicular magnetic induction component for tag (B_{min}=740 nT), which is located at distance 0,5 m from the centre on axis of symmetry of RWD antenna surfaces with equal areas: a) circular loop, b) rectangle loop - *a/b*=0.028

4.4 Conditions of identification conducted nearby objects which disturb data transfer

Prior considerations of the energy transmission through the magnetic field generated within the RWD antenna have related to the no disturbed environment that is characterized only by a magnetic permeability of free space μ_0 (relative magnetic permeability of air -

μ_r=1.00000036 - is assumed with value equal 1). However, sometimes it is necessary to take into consideration the impact of objects placed into a magnetic field of RWD antenna on changes in the magnetic induction vector at the point of identifiers location. The need for carrying out an identification process of ferromagnetic objects or these which are located near to ferromagnetic materials can be given as an example (Fig. 14-a).

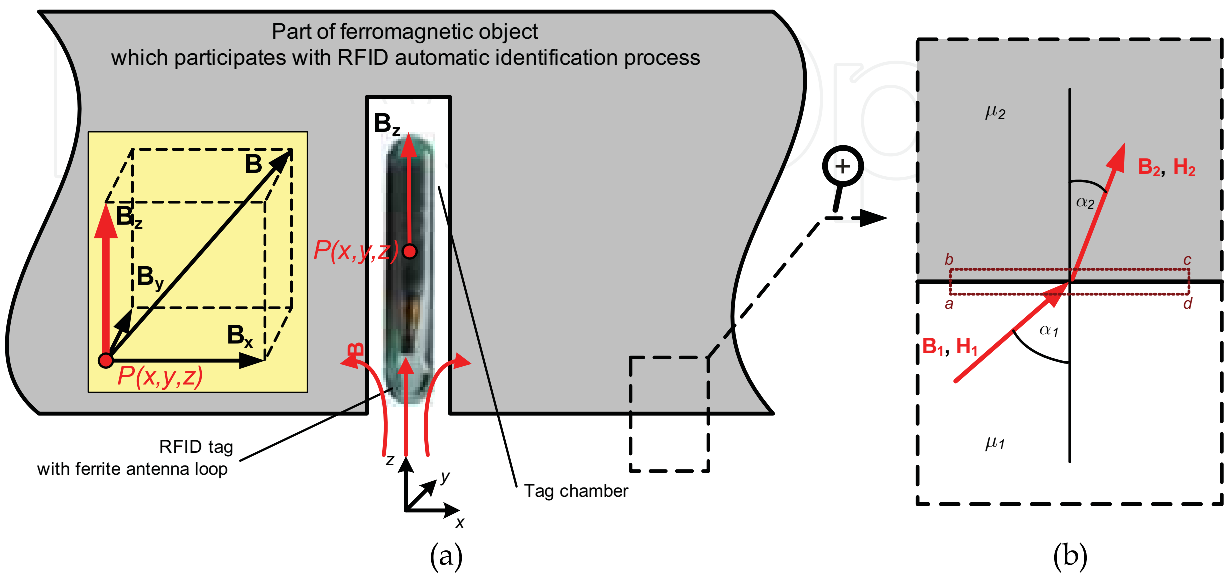

Fig. 14. Identification of the object distorting a data transmission: a) orientation of tag attached to ferromagnetic elements with reference to the RWD antenna loop, b) the magnetic field at the boundary of environments

A knowledge about strongly influenced (with respect to the system without ferromagnetic materials) direction and sense of the magnetic induction vector in the area in which there are ferromagnetic objects allows the correct analysis of a transponder orientation in the magnetic field of RWD antenna loop (see 4.2). It also gives reason for a proper determination of the tag interrogation zone and thus to fulfil the field conditions of specific work environment.

If the rectangular contour *abcd* (Fig. 14-b) will be assumed on the boundary of the ferromagnetic object then the fallowing equation is fulfilled in the open circuit for the vector of magnetic field strength **H**:

$$\oint_l \mathbf{H} \cdot \mathrm{d}\mathbf{l} = 0 \tag{39}$$

Assuming that the lengths of sides (rectangle with perimeter *l*) *ab* and *cd* are negligibly small in relation to *bc* and *da*, from equation (39) follows the equality:

$$H_1 \sin\alpha_1 = H_2 \sin\alpha_2 \tag{40}$$

On the other hand, for the area where there is no current flow and the equation of the vector magnetic induction **B** is satisfied:

$$\oint_S \mathbf{B} \cdot \mathrm{d}\mathbf{S} = 0 \tag{41}$$

and assuming that there is negligible small surface S of rectangle located in *abcd* contour, perpendicular to the surface of figure 14-b, it is possible to write:

$$B_1 \cos\alpha_1 = B_2 \cos\alpha_2 \tag{42}$$

It follows from equation (40) that there is continuity of tangential component of the vector **H** at the environment boundary, while from equation (42) - continuity of normal component of vector **B**. On the base of the fallowing equation of material:

$$\mathbf{B} = \mu\mathbf{H} \tag{43}$$

boundary conditions (40) and (42) can be presented in the form of the vector refraction law for the magnetic field:

$$\frac{\mu_1}{\mu_2} = \frac{tg\alpha_1}{tg\alpha_2} \tag{44}$$

Equation (44) is true with assumption that the identification system from the Fig. 14-a is placed in the *z-x* plane, that is there is not its shift in the *y*-axis direction. In the identification process carried out nearby objects disturbing the magnetic field of RWD antenna loop it is better to use the magnetic vector potential **A** when determining induction **B** in the tag placement area. The dependences (40) and (42) show that there is continuity of vector potential at the boundary in the Fig. 14 where the equation is satisfied:

$$\mathbf{B} = \nabla \times \mathbf{A} \tag{45}$$

After using equations (43), (45) and the expression describing the area of tag placement without current flow, $\nabla \times \mathbf{H} = 0$, the relationship was obtained:

$$\Delta\mathbf{A} = 0 \tag{46}$$

Relationship (46) is the vector Laplace equation which describes the distribution of vector potential in the placement area of tag. So the problem of the correct location for the tag placed nearby ferromagnetic objects is reduced to such a boundary problem which has to be solved. Moreover, in order to meet field condition requirements, it is necessary to find out such an tag orientation in the magnetic field of RWD antenna loop (see 4.2) at which the condition of minimum magnetic induction value is fulfilled for the given tag. This implies the need for determining the perpendicular component of magnetic induction vector at the location point of tag which will be used to mark the object.

In the most general case, the lack of symmetry indicates the need to solve the system of three Laplace equations formulated for each of the Cartesian coordinates *x, y* and *z*:

$$\Delta\mathbf{A} = \begin{pmatrix} \frac{\partial^2 A_x}{\partial x^2} + \frac{\partial^2 A_x}{\partial y^2} + \frac{\partial^2 A_x}{\partial z^2} \\ \frac{\partial^2 A_y}{\partial x^2} + \frac{\partial^2 A_y}{\partial y^2} + \frac{\partial^2 A_y}{\partial z^2} \\ \frac{\partial^2 A_z}{\partial x^2} + \frac{\partial^2 A_z}{\partial y^2} + \frac{\partial^2 A_z}{\partial z^2} \end{pmatrix} = 0 \tag{47}$$

Analytical methods for solving these issues (e.g. separation of variables method) often can not be used because of complicated shapes of ferromagnetic objects which sometimes affect the identification process very strong. Then, it is necessary to use numerical methods and specialized software that allows to define the problem, enter boundary conditions and obtain convergent results in quick way.

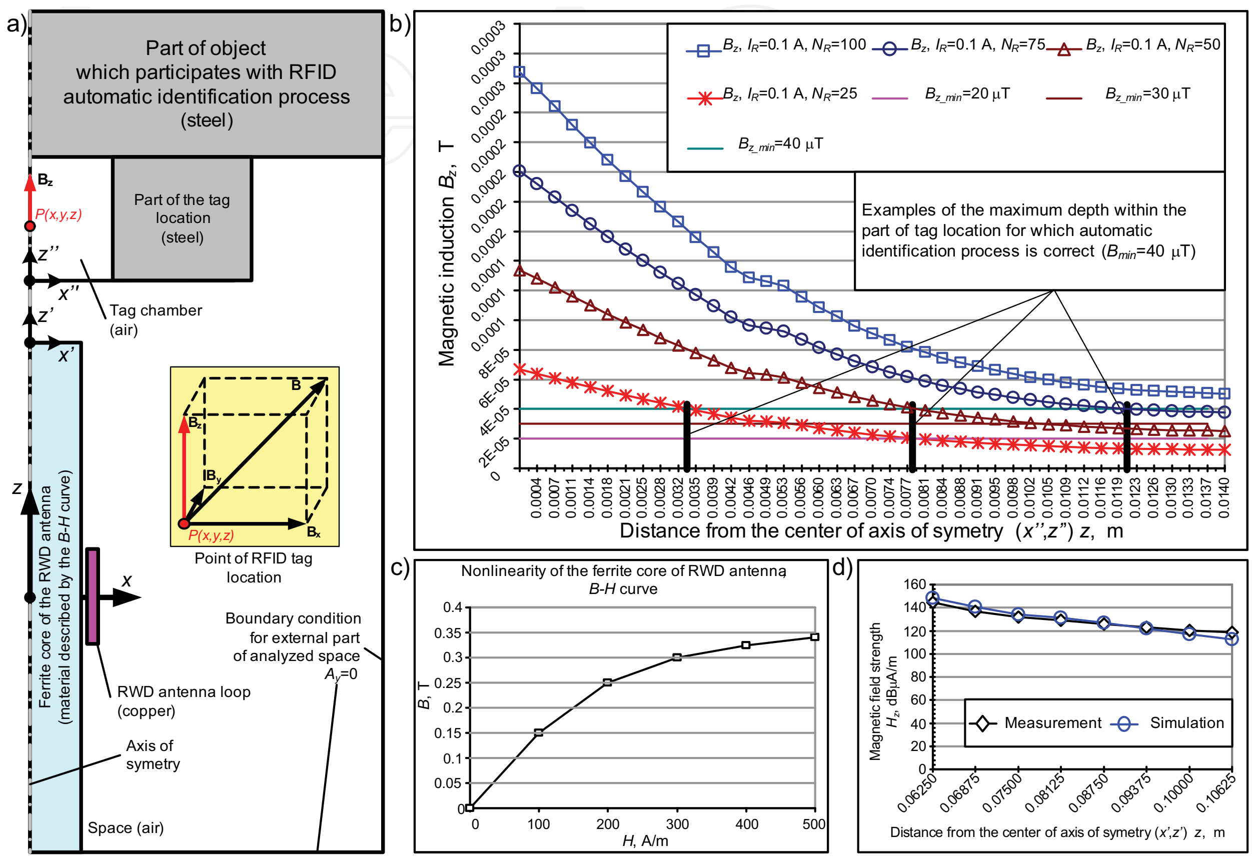

Fig. 15. FEM model for an example of RFID identification of ferromagnetic object:
a) axially symmetric model, b) calculation results from ANSYS software – component B_y inside a mounting element chamber, c) the curve **B-H** for the ferrite core of RWD antenna, d) experimental verification of model

An example of RFID identification process for ferromagnetic object is shown in the Fig. 15. It is necessity to use a directional antenna in order to read information from tag working in this system. The antenna has to stably operate at resonant frequency of RFID system. Placing the antenna close to the ferromagnetic object determines the need of the maximum distance between the RWD loop and the object and using small antennas. It makes impedance component contributed by the object to the electrical circuit of RWD antenna loop lees significant. Barriers to the operation of antenna units in the field of electrical conditions were presented in (Jankowski-M. & Kalita, 2008 and 2009).

Using a small loop, which is about a few centimetres from the identified object, does not allow for stable operation of the RWD antenna unit. It is also impossible to meet the requirement for the minimum value of magnetic induction for one or more tags. For this reason, it is necessary to use an antenna with a ferrite rod, which forms the magnetic amplifier (magnetic core). Adoption of the previous assumptions according to the RWD antenna operation (4.1) makes possible to develop a simulation model with using the finite element method. The model has been analyzed in the magneto-static field (Fig. 15-a).

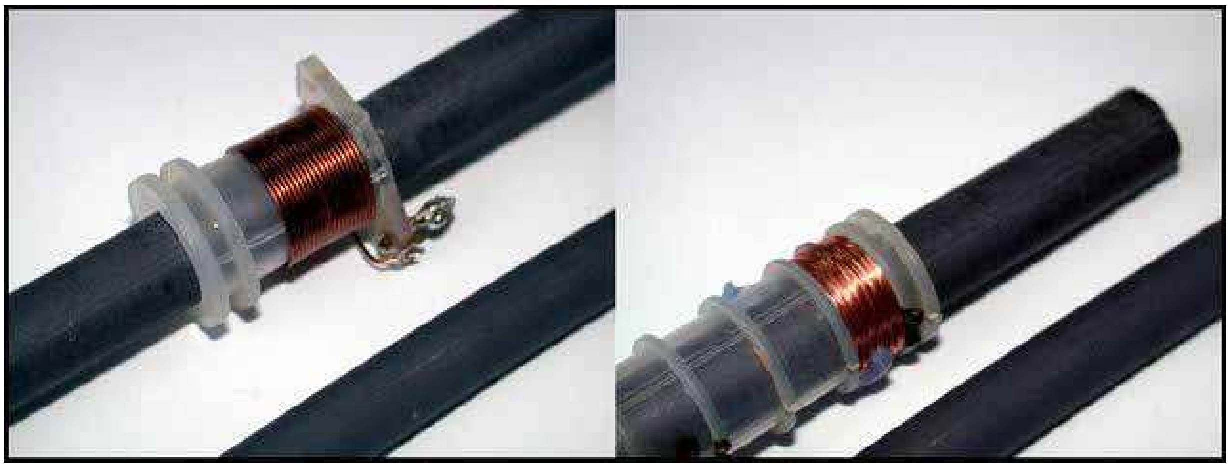

Fig. 16. Measuring samples of ferrite RWD antenna

The FEM model that was built for the ANSYS software (Fig. 15-c,d) was verified by simulating and measuring the H_z component of magnetic field strength for the tested antenna (Fig. 16). The antenna was made by winding 100 turns of wire with a diameter of 0.3 mm round the ferrite cores with a length of 0.125 m, diameter of 0.005 m and initial permeability of 20. Highlighted the discrepancy between simulation results and measurements was at the level of 3-4 %, in the worst case. It is due to conducting simulation process of magnetic field in a long air gap occurring between the metal elements.

The results (Fig. 15-b) clearly show the maximum value of depth within the mounting element of identifier. The value determines the range of depth where the tag with precisely fixed minimum value of magnetic induction should be placed. Ferromagnetic cylinder with a drilled hole constituted attachment part of the transponder.

Same of the magnetic induction flux and vector observations in the tag placement area (Fig. 17-a,b) show the possibility of finding the correct set of system components for the purpose of carrying out the identification process. It is possible with proper placing RWD antenna or by re-orientating the antenna loop.

Developed FEM simulation model is widely discussed in publications (Jankowski-M., 2007). It can provide a basis for synthesis of solutions in RFID identification systems modified in its construction. In particular it is useful in industrial logistics systems, presented in Fig. 18 and in publication (Fitowski et al., 2005) as an examples. In the first case (Fig. 18-a), a method of passive RFID tag affixing on the flange of technical gas cylinders is presented. The method was developed in Department of Electronic and Communication Systems of Rzeszów University of Technology within the confines of a whole computer system for RFID identification of gas cylinders. The presented method has been also used practically in an innovative and unique design of the RFID system for collection of mining equipment in underground environment - Fig. 18-b. Powered roof support units pose difficult objects in identification process due to the metal construction and adverse operating conditions such as vibration, stress, corrosive environment, very high humidity and dust.

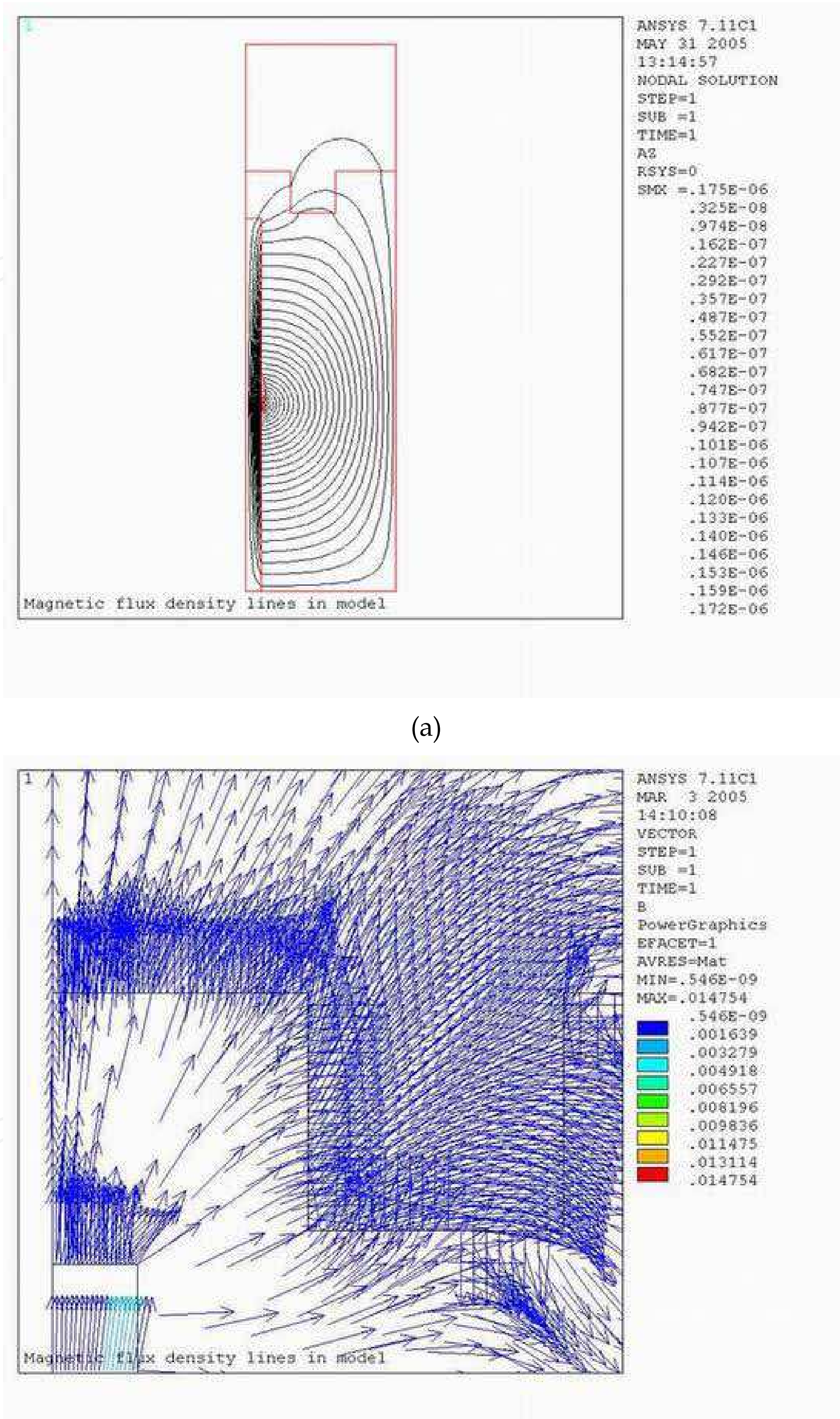

(a)

(b)

Fig. 17. Examples of simulation results in ANSYS software for the modeled identification system: a) magnetic induction flux in the system, b) normalized magnetic induction vectors nearby the identifier chamber

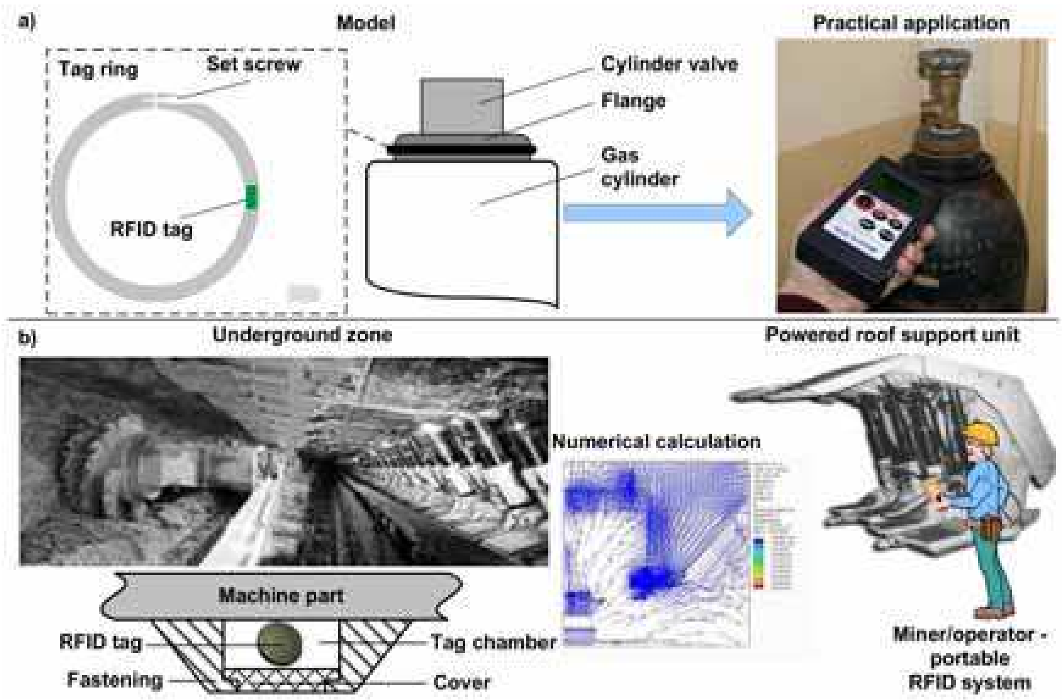

Fig. 18. Parts of a computer systems: a) RFID identification of gas cylinders,
b) RFID data collection in underground environment

5. Conclusion

The operation of passive anticollision RFID systems with inductive coupling is characterized by the interrogation zone, which is estimated in any direction of 3D space for group of electronic tags. The elements of algorithm for interrogation zone estimation in inductive coupled anticollision RFID identification system, taking into consideration the field aspects of operation conditions has been presented in this chapter. The special procedure of theoretical and experimental investigations, designed and made in Department of Electronic and Communication Systems, Rzeszów University of Technology, allows to determinate the functional efficiency of whole anticollision RFID system for all typical operating frequencies. The efficiency is just defined as the interrogation zone for group of *n*-tags and selects process of automatic identification on different economic and public activity in industry, commerce, science, medicine and others. This procedure is the last and most important stage of algorithm of synthesis of RWD and tag antenna set for the anticollision RFID system with inductive coupling. This is only preceded by stages, where the selection of RWD and tags along with antenna sets is carrying out. The final solution is calculation of the antenna unit array - based on Monte Carlo method and computer program with use of Mathcad (Jankowski-M., 2007) - with taking into consideration the algorithm of its synthesis according to equations, which have been determined during the synthesis of its electric model (Jankowski-M. & Kalita, 2008).
Paying attention to the maximum work distance between elements of the RFID system, in particular for systems working in the RFID far field, it is necessary to estimate the simulated and built antenna set RWD-tags in relation to the obligatory normalizations of communication and EMC. The electro-magnetic compatibility problems and current legal status for selected frequency bands used in different dedicated solutions (i.e. the animals'

identification, access control and objects identification in logistic process) have been taken into account in detail. The method of synthesis interrogation zone in accordance with EMC has enabled exact estimation of the non-interference of data transmission area (for write and read process) between RWD and electronic tags.

6. References

Åhlström, L. (2005). Flight RFID now boarding, *Global Ident. Magazine*, Vol. October, pp. 22-25

Bhatt, H.; Glover, B. (2006). *RFID Essentials*, O'Reilly, ISBN 978-0596009441

Cichos, S. (2002). Performance Analysis of Polymer Based Antenna-Coils for RFID, *IEEE Polytronic Conference*, pp.120-124, June 23-26, 2002, Zalaegerszeg, Hungary

Dobkin, D.; Wandinger, T. (2005). A Radio-Oriented Introduction to RFID-Protocols, Tags and Applications, *High Frequency Electronics*, Vol. 4, No. 6, pp. 32-46

Donaldson, J. (2009). Plugging profit leaks in the apparel sector, *ID World*, Vol. June, pp. 40-42

EN 50357 (2001). *Evaluation of human exposure to electromagnetic fields from devices used in Electronic Article Surveillance (EAS), Radio Frequency Identification (RFID) and similar applications*, IEC

EN 50364 (2001). *Limitation of human exposure to electromagnetic fields from devices operating in the frequency range 0 Hz to 10 GHz, used in Electronic Article Surveillance (EAS), Radio Frequency Identification (RFID) and similar applications*, CENELEC

ERC Rec. 70-03 (2008). *Relating to the use of short range devices (SRD)*, Edition of May 2008

ETSI EN 300 330-1 (2006). *Electromagnetic compatibility and Radio spectrum Matters (ERM); Short Range Devices (SRD); Radio equipment in the frequency range 9 kHz to 25 MHz and inductive loop systems in the frequency range 9 kHz to 30 MHz; Part 1: Technical characteristics and test methods*. V1.5.1

ETSI EN 300 330-2 (2006). *Electromagnetic compatibility and Radio spectrum Matters (ERM); Short Range Devices (SRD); Radio equipment in the frequency range 9 kHz to 25 MHz and inductive loop systems in the frequency range 9 kHz to 30 MHz; Part 2: Harmonized EN under article 3.2 of the R&TTE Directive*, V1.3.1

Finkenzeller, K. (2003). *RFID Handbook: Fundamentals and Applications in Contactless Smart Card and Identification*, Second Edition, Wiley, ISBN 978-0470844021, New York

Fitowski, K., Stankiewicz, J.; Jankowski, H.; Szczurkowski, M.; Jankowski-Mihułowicz, P.; Warzecha, M.; Krzak, Ł.; Worek, C.; Meder, A. (2005). RFID collection system of mining equipment in underground environment, *IV International Conference New electrical and electronic technologies and their industrial implementation (NEET'05)*, pp. 250-253, ISBN 83-87414-87-5 , June 21-24, Zakopane, Poland

Flores, J.; Srikant, S.; Sareen, B.; Vagga A. (2005). Performance of RFID tags in near and far field, *IEEE International Conference Wireless Communications (ICPWC'05)*, pp. 353-357, ISBN 0-7803-8964-6, 23-25, January 2005, New Delhi, India

Halliday, D.; Resnick, R.; Walker, J. (2004). *Fundamentals of Physics*, 7th Edition, Wiley, ISBN 978-0471216438, New York

Harrison, R. (2009). A practice of vetting RFID, *Global Ident. Magazine*, Vol. July, pp. 18-20

IEC 62369 (2008). *Evaluation of human exposure to electromagnetic fields from short range devices (SRDs) in various applications over the frequency range 0 GHz to 300 GHz - Part 1: Fields* *produced by devices used for electronic article surveillance, radio frequency identification and similar systems*, IEC

Jankowski-Mihułowicz, P.; Kalita, W. (2009). Efficiency of Tag Antenna Unit in Anticollision Radio Frequency Identification Systems with Inductive Coupling, *Acta Electrotechnica et Informatica*, Vol. 9, No. 2. pp. 3-7, ISSN 1335-8243

Jankowski-Mihułowicz, P.; Kalita, W.; Pawłowicz, B. (2008). Problem of dynamic change of tags location in anticollision RFID systems, *Microelectronics Reliability*, Vol. 48, Issue 6, pp. 911-918

Jankowski-Mihułowicz, P.; Kalita, W. (2008). Problem of Interrogation Zone Synthesis in Anticollision Radio Frequency Identification Systems, *31th International Spring Seminar on Electronics Technology Reliability and Life-time Prediction (ISSE'08)*, pp. 647-652, ISBN 978-9630649155, May 7-11, 2008, Budapest, Hungary

Jankowski-Mihułowicz, P. (2007). Creation conditions of antenna array efficiency of anticollision Radio Frequency Identification systems with inductive coupling, *PhD dissertation*, AGH University of Science and Technology, Kraków

Jankowski-Mihułowicz, P.; Kalita, W. (2004). Passive tag supply work in radio frequency identification system, *Elektronika*, Vol.1, pp. 26-30, ISSN 0033-2089

Microchip (2004). *MicroID 125 kHz 13.56 MHz RFID System Design Guide*

Paret, D. (2005). *RFID and Contactless Smart Card Applications*, Wiley, ISBN 978-0470011959

Steden, G. (2005). A business case for RFID, *Global Ident. Magazine*, Vol. December, pp. 58-61

Wolfram, G.; Gampl. B.; Gabriel, P. (2008). *The RFID Roadmap: The Next Steps for Europe*, Springer, ISBN 978-3540710189

Wyld, D. C. (2009). Reinventing trash, *Global Ident. Magazine*, Vol. March, pp. 58-62

Wyld, D. C. (2005). RFID in the public sector, *Global Ident. Magazine*, Vol. October, pp. 46-51

Yan, L.; Zhang, Y.; Yang, L. T.; Ning, H. (2008). *The Internet of Things: From RFID to the Next-Generation Pervasive Networked Systems*, Auerbach, ISBN 978-1420052817

Yeh, M.-K.; Jiang, J.-R.; Huang, S.-T. (2009). Adaptive Splitting and Pre-Signaling for RFID Tag Anti-Collision, *Computer Communications*, Vol. 32, Issue 17, pp. 1862-1870, ISSN 0140-3664

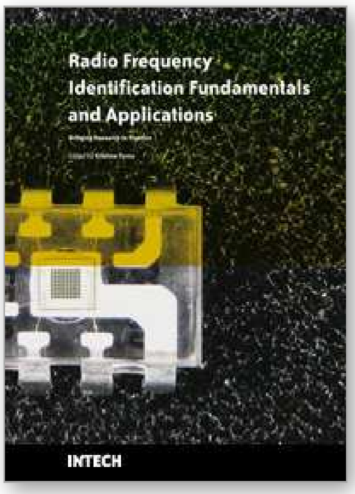

Radio Frequency Identification Fundamentals and Applications Bringing Research to Practice

Edited by Cristina Turcu

ISBN 978-953-7619-73-2
Hard cover, 278 pages
Publisher InTech
Published online 01, February, 2010
Published in print edition February, 2010